Published in final edited form as:
DNA Repair (Amst). 2011 November 10; 10(11): 1164–1173. doi:10.1016/j.dnarep.2011.09.002.

PIF1 disruption or NBS1 hypomorphism does not affect chromosome healing or fusion resulting from double-strand breaks near telomeres in murine embryonic stem cells

Gloria E. Reynolds[a], **Qing Gao**[b], **Douglas Miller**[a], **Bryan E. Snow**[c], **Lea A. Harrington**[d], and **John. P. Murnane**[a,*]

[a]Department of Radiation Oncology, University of California San Francisco, 2340 Sutter Street, San Francisco, CA 94143-1331

[b]Whitehead Institute for Medical Research, Cambridge, MA 02142

[c]Ontario Cancer Institute, Campbell Family Institute for Breast Cancer Research, 620 University Avenue, Room 706, Toronto M5G 2C1, Canada

[d]Wellcome Trust Centre for Cell Biology, University of Edinburgh, Edinburgh, Scotland EH9 3JR

Abstract

Telomerase serves to maintain telomeric repeat sequences at the ends of chromosomes. However, telomerase can also add telomeric repeat sequences at DNA double-strand breaks (DSBs), a process called chromosome healing. Here, we employed a method of inducing DSBs near telomeres to query the role of two proteins, PIF1 and NBS1, in chromosome healing in mammalian cells. PIF1 was investigated because the PIF1 homolog in *S. cerevisiae* inhibits chromosome healing, as shown by a 1000-fold increase in chromosome in PIF1-deficient cells. NBS1 was investigated because the functional homolog of NBS1 in *S. cerevisiae*, Xrs2, is part of the Mre11/Rad50/Xrs2 complex that is required for chromosome healing due to its role in the processing of DSBs and recruitment of telomerase. We found that disruption of *mPif1* had no detectable effect on the frequency of chromosome healing at DSBs near telomeres in murine embryonic stem cells. Moreover, the Nbs1$^{\Delta B}$ hypomorph, which is defective in the processing of DSBs, also had no detectable effect on the frequency of chromosome healing, DNA degradation, or gross chromosome rearrangements (GCRs) that result from telomeric DSBs. Although we cannot rule out small changes in chromosome healing using this system, it is clear from our results that knockout of PIF1 or the Nbs1$^{\Delta B}$ hypomorph do not result in large differences in chromosome healing in murine cells. These results represent the first genetic assessment of the role of these proteins in chromosome healing in mammals, and suggest that murine cells have evolved mechanisms to ensure the functional redundancy of Pif1 or Nbs1 in the regulation of chromosome healing.

Keywords

Chromosome fusion; Chromosome healing; Chromosome instability; Double-strand break; NBS1; PIF1; Telomere

Corresponding author: John P. Murnane, Tel: (415) 476 9083, Fax: (415) 476 9069., jmurnane@radonc.ucsf.edu.

1. Introduction

Telomeres in mammalian cells are composed of a six base pair repeat sequence and associated proteins that together form a cap that protects the ends of chromosomes [1]. The telomeric repeat sequences are added by the enzyme telomerase to compensate for the loss of DNA from the ends of chromosomes during cell division. Telomeres are maintained in germ line cells and embryonic stem (ES) cells, which express telomerase, but shorten with age in somatic cells due to insufficient expression of telomerase. Telomere shortening limits the lifespan of somatic cells, because the eventual loss of telomere function results in replicative cell senescence or apoptosis. Cells that lose the ability to senesce continue to undergo telomere shortening, eventually resulting in extensive chromosome fusion. Thus, for cancer cells to become immortal, they must regain the ability to maintain telomeres, either through the reactivation of telomerase or the expression of an alternative pathway involving recombination that is found in some cancer cells [2].

Studies in yeast have demonstrated that telomeres can be restored on the ends of broken chromosomes through the *de novo* addition of telomeric repeat sequences by telomerase, a process called chromosome healing [3]. Chromosome healing *S. cerevisiae* is inhibited by Pif1, which has been proposed to be a mechanism that prevents chromosome healing from interfering with double-strand break (DSB) repair [4]. Mutations in *PIF1* can cause up to a 1000-fold increase in chromosome healing, as well as an increase in telomere length, demonstrating that Pif1 is a negative regulator of telomerase [5, 6]. The effect of Pif1 on telomere length is mediated by its interaction with catalytic subunit of telomerase, TERT (ScEst2), since mutations in Est2 that affect Pif1 binding also result in telomere elongation [7]. Chromosome healing in *S. cerevisiae* requires the Mre11/Rad50/Xrs2 (MRX) complex [8], possibly due to a failure in processing of DSB or the role of the MRX complex in the recruitment of telomerase to telomeres [8, 9]. The extensive resection of DSBs can also inhibit chromosome healing, as demonstrated by the fact that chromosome healing is greatly increased by deficiencies in Exo1 and Sgs1 [10, 11]. This effect is independent of Pif1, because the combination of mutations in *PIF1* with mutations in *EXO1* and *SGS1* increases chromosome healing to 50% of the cells experiencing a DSB [10].

Chromosome healing also occurs in mammalian cells. Terminal deletions resulting from chromosome healing in germ line cells are responsible for human genetic disease [12–14]. An *in vitro* assay using oligonucleotide primers based on a site of chromosome healing in alpha thalassemia patients demonstrated that telomerase can perform *de novo* telomere addition using only a single nucleotide of homology with the telomerase RNA [15, 16]. However, despite the fact that chromosome healing can occur in germline cells, it has not been observed at random interstitial DSBs in immortal mammalian cell lines in culture [17–19]. Moreover, the presence of telomerase did not affect the response to ionizing radiation in murine embryo fibroblasts, suggesting that chromosome healing does not occur at most DSBs [20]. Therefore, as in yeast, chromosome healing appears to be tightly regulated in mammalian cells.

Although chromosome healing is a rare event at DSBs at most locations, it is a common event in response to DSBs near telomeres in murine ES cells [21, 22]. DSBs induced with the I-SceI endonuclease in the pPPT2-tel plasmid located adjacent a telomere resulted in three types of events in approximately equal proportions: the loss of the plasmid, chromosome healing, and sister chromatid fusion leading to chromosome instability [21–23]. Sister chromatid fusions nearly always occurred in combination with degradation at the DSB, often resulting in all of the plasmid DNA on one of the sister chromatids. Although they could not be analyzed, it is likely that the cells experiencing complete loss of the

plasmid also underwent sister chromatid fusions, but with degradation of the plasmids on both sister chromatids. In contrast, chromosome healing nearly always occurred at the site of the DSB. Chromosome healing therefore prevents degradation, sister chromatid fusion, and chromosome instability, leading to the hypothesis that chromosome healing serves as an important mechanism for preventing chromosome instability due to DSBs near telomeres [21]. As in yeast, telomerase is involved in chromosome healing in murine ES cells, although ES cell lines that have acquired the ability to maintain telomeres through a telomerase-independent mechanism can also perform chromosome healing [21].

In the current study we have investigated whether pathways that influence chromosome healing in yeast also influence chromosome healing in mammalian cells. These studies involve the analysis of the frequency of chromosome healing at DSBs near telomeres in murine ES cells that are homozygous for knockout of PIF1 or that contain a hypomorphic mutation in Nbs1. ES cell lines homozygous for a disrupted *mPif1* allele were analyzed to determine whether mammalian PIF1, which like *S. cerevisiae* Pif1 binds to TERT [24, 25], is also involved in the regulation of chromosome healing. The ES cell lines homozygous for the $Nbs1^{\Delta B}$ hypomorphic gene ($Nbs1^{\Delta B/\Delta B}$) were investigated because Nbs1 is the functional homolog of *S. cerevisiae* Xrs2, and also forms a complex with Mre11 and Rad50 (MRX), which is involved in the processing of DSBs [26]. The $Nbs1^{\Delta B}$ hypomorph lacks the FHA domain that is involved in recruitment of DNA repair proteins to DSBs [26, 27]. Although cells homozygous for the $Nbs1^{\Delta B}$ hypomorph activate phosphorylation of Atm and p53 in response to DSBs, Atm function is compromised, as demonstrated by an increased sensitivity to DSBs, failure to phosphorylate Chk2, and lack of a S phase or G2 arrest in response to DSBs [28–30]. The ES cell lines lacking Pif1 or containing the Nbs1 hypomorph also contain the pPPT2-tel plasmid located adjacent to a telomere. As we have shown previously, the pPPT2-tel plasmid enables one to monitor the consequences of DSBs located near telomeres. The pPPT2-tel plasmid contains both selectable marker genes and an I-SceI endonuclease recognition site for selectively introducing DSBs. Following the introduction of DSBs with I-SceI endonuclease, the ES cell lines were analyzed for the frequency of large deletions, GCRs, and chromosome healing.

2. Materials and methods

2.1 Plasmids

The pPPT2-tel plasmid used for generation of the ES cell clone 10P and 10P mice [31] contains a Puromycin resistance ($Puro^r$) gene with a Herpes simplex virus thymidine kinase (HSV-tk) promoter for positive selection with puromycin, an HSV-tk gene preceded by a murine 3-phosphoglycerate kinase (PGK) gene promoter for negative selection in ganciclovir, and 0.8 kbp of telomeric repeat-containing DNA for seeding the formation of new telomeres following chromosomal integration.

2.1 Establishment of ES cell lines and transgenic mice containing telomeric plasmid DNA

The method for establishment and characterization of murine ES cell clones containing telomeric plasmids has been described previously [22, 23]. The ES cell clone 10P was generated by transfection of ES cells with the linearized pPPT2-tel plasmid containing telomeric repeat sequences on one end, and selection of clones containing the stably-integrated plasmid with puromycin. The puromycin-resistant ES cell clones were then screened by Southern blot analysis for clones in which a single copy of the plasmid had become the new telomere on a chromosome, as indicated by the large size of the band containing the telomeric repeat sequences. The telomeric integration site was then confirmed by fluorescent *in situ* hybridization, sequencing of the rescued plasmid sequences and adjacent cellular DNA, and Southern blot analysis following digestion with BAL31 nuclease

[31]. The location of the newly seeded telomere was determined by sequence analysis of host DNA to be 1.4 Mbp from the original end of chromosome 11 (Genbank Accession No. EF503725). The 10P transgenic murine strain was established from the 10P ES cell clone in conjunction with the UCSF Transgenic Core Facility as described previously [32]. Briefly, ES cells were injected into blastocysts from C57BL/6J mice, and the resulting chimeric mice were bred with C57BL/6J mice to generate the 10P murine strain containing the telomeric plasmid DNA. PCR, using primers specific for the HSV-tk gene, and Southern blot analysis, using a pNTPΔ probe, was used to analyze tail DNA to identify mice that contained the telomeric plasmid sequences, as described previously for analysis of ES cell lines [22].

2.3 Isolation of PIF1 knockout and NBS1 hypomorphic ES cell lines containing pPPT2-tel

The Pif1 knockout and NBS1$^{\Delta B/\Delta B}$ ES cell lines employed in this study were created by crossing the 10P mouse with mouse strains containing either the Pif1 knockout or NBS1$^{\Delta B}$ hypomorphic alleles. The methods for generation and characterization of the Pif1 knockout [24] and Nbs1$^{\Delta B}$ hypomorphic mice [28] have been described previously. The approach used to generate these ES cells lines involved first identifying male mice that were heterozygous for the Pif1 knockout or NBS1$^{\Delta B}$ hypomorphic alleles, and also heterozygous for the pPPT2-tel plasmid. These male mice were then crossed with female mice that were heterozygous for the Pif1 knockout or Nbs1$^{\Delta B}$ hypomorphic allele. Three days post coitus, the female mice were sacrificed, the blastocysts isolated, and the ES cell lines were established and genotyped by polymerase chain reaction (PCR). Genotype analysis was then performed (Figure S1), using PCR primers for the wild type *PIF1* gene, the *PIF1* knockout gene, and the pPPT2-tel plasmid. Using this protocol, we identified four wild type 10P ES cell lines, 10PWT-FA, 10PWT-CP, 10PWT-FB, and 10PWT-BA, and two 10P ES cell lines that were homozygous for the Pif1 knockout allele, PIF-2H and PIF-9A. The control and Pif1 knockout ES cell lines were not all isolated from the same litter. However, the genetic background of the ES cell lines is genetically homogeneous, since the 10P mice had been back-crossed 6 times with C57BL/6J mice, and the Pif1 knockout mice had been back-crossed 8 times with C57BL/6J mice [24]. A similar approach was used to identify two 10P cell clones that were homozygous for the Nbs1$^{\Delta B}$ hypomorphism (Nbs1$^{\Delta B/\Delta B}$), NBS-7C and NBS-8H (data not shown).

2.4 Isolation of ES cell lines from transgenic/knockout mice

The method for isolation of ES cell lines from mice was performed as described previously [31, 33]. Briefly, blastocysts were collected by flushing out the uterine horns of 3.5-day postcoitum mice with M2 media (Sigma). The blastocysts were then transferred individually into 10-mm tissue culture wells containing a layer of PMEF feeder cells (Specialty Media) in ES media, and were cultured at 37°C in a 5% v/v CO_2 humidified incubator for approximately 10 days. The inner-cell-mass-derived outgrowths were treated with trypsin and transferred into new tissue culture wells containing PMEF feeder cells. After 4 days in culture, the ES-cell-like clumps were selected, expanded, and frozen for future use. The ES cell lines were then screened for pPPT2-tel using primers specific for the HSV-tk gene [22], wild type and knockout murine Pif1 alleles [24], and murine wild type Nbs1 and Nbs1$^{\Delta B}$ hypomorpic alleles [28]. ES cells (or mice) that were homozygous for the telomeric pPPT2-tel integration were not detected; the formation of the new telomere in ES cell clone 10P generated a 1.4 Mbp terminal deletion with the loss of approximately 20 genes, likely resulting in inviability (G.E.R., B.E.S., unpublished).

2.5 Analysis of PIF1 expression by rt-PCR

The analysis of gene expression by real time quantitative PCR (rt-PCR) was performed using total RNA prepared using a Midi purification kit (Invitrogen, Carlsbad CA). Samples were treated with DNA-free kit (Ambion, Austin TX) to remove traces of genomic DNA

contamination. Preparation of cDNA from these RNA samples was performed as described previously [34] with the following modifications: reactions were incubated for 40 min at 48 °C, using 7.5 mM $MgCl_2$, 1 mM dNTPs, 5 μM hexamers (Random Primers, Invitrogen), and 2.5 U/μl of M-MLV reverse transcriptase (Invitrogen, Carlsbad CA). To control for genomic DNA contamination, a mock cDNA preparation of each sample was prepared in a parallel reaction without the presence of the reverse transcriptase. Rt-PCR was performed in triplicate by the UCSF Cancer Center Genome Analysis core facility using an ABI 7700 Prism real-time thermocycler (PE Biosystems, Foster City, CA) as described previously [32]. The primers employed for *PIF1* were 5′-TGACACTAAGAGGTCTGGACAGG-3′ and 5′-TGCTAGAAGGCATCTCCAATG-3′, and the probe for *PIF1* was 5′-6FAM-CGGAGCGCATAAGTCACAGAAAATCG-IABLFQ-3′. The level of gene expression was determined relative to expression of the L19 gene, using primers 5′-CCAAGAAGATTGACCGCCATA-3′ and 5′-GTCAGCCAGGAGCTTCTTGC-3′, and the probe 5-FAM-CATCCTCATGGAGCACATCCACAAGC-IABLFQ-3′.

2.6 Transfection with I-SceI and selection for loss of the HSV-tk gene

Expression of I-SceI endonuclease was achieved by transient transfection with the pCBASce plasmid. pCBASce contains the I-SceI gene with a chicken β-actin promoter, and has been shown previously to provide a high efficiency of cutting at I-SceI sites in mammalian cells [35]. Thirty micrograms of pCBASce was electroporated into 5×10^6 cells. The next day, the cells were plated at 2×10^5 cells per 100 mm tissue culture dish, and after culturing for 6 days to allow turnover of existing *HSV-tk* [36, 37], selection was performed using medium containing either 2 μM ganciclovir alone, or a combination of 2 μM ganciclovir and 2 μg/ml puromycin. Selection with ganciclovir alone was used for analysis of the frequency of the different types of events, while selection with both ganciclovir and puromycin was used for sequence analysis of recombination junctions. Selection with puromycin was used to insure that the $puro^r$ gene was retained, making it easier to locate the recombination junction. Individual colonies were then selected for analysis after approximately 2 weeks.

2.7 Southern blot analysis

Genomic DNA was purified by high-salt extraction. Cell pellets were washed and resuspended in STE (0.02 M Tris HCl, 0.01 M EDTA, 0.1 M NaCl, pH 8.5). Sodium dodecyl sulfate (Sigma) was then added to a final concentration of 0.5% w/v and the lysed cells were heated at 60°C for 10 minutes. RNAse A (Sigma) was added to a final concentration of 50 μg/ml and the lysed cells incubated at 37°C for 4 hours, followed by the addition of Proteinase K (Sigma) to a final concentration of 32 μg/ml and incubation overnight at 37°C. 5M NaCl was then added to a final concentration of 1.4 M, and the samples chilled on ice for 30 minutes. The lysis solution was then centrifuged at 3,000 g, and the clear DNA solution removed using a wide-bore pipet. The DNA was precipitated with 0.7 volumes of isopropanol, and removed by capture with a sterile micropipet tip. The precipitated DNA was then added to a 1.5 ml Eppendorf tube containing 70% v/v ethanol and pelleted at maximum speed with an Eppendorf 5415 centrifuge. After pouring off the ethanol solution, the DNA pellet was dried and resuspended in TE buffer (0.1 M NaCl, 0.01 M TrisHCl, pH 7.5).

Digestion of DNA with restriction enzymes and BAL31 nuclease was performed following the manufacturer's recommendations (New England Biolabs). Standard agarose gel electrophoresis was performed as described previously [23]. PFGE was performed using 1% w/v agarose in 0.5 × TBE (0.045M Tris-borate, 0.001M EDTA), at 150V, 10°C, and pulsed at 2 to 5 second intervals for PFGE. Southern blot analysis involved depurination of DNA by treatment with 0.25 M HCl for 20 minutes, denaturation in 0.5 M NaOH/1.5 M NaCl for 30 minutes, neutralization in 1 M Tris/1.5 M NaCl pH 7.5 for 30 minutes, and transfer onto

a charged nylon Hybond-N+ membrane (Amersham) in 10 × SSC (1.5 M NaCl/0.15 M Na Citrate, pH 7.0) using a vacuum transfer apparatus (Pharmacia). Prehybridization for 30 minutes and hybridization overnight were performed at 65°C in roller bottles in hybridization buffer (0.25 M Na phosphate buffer, pH 7.2, 1 mM EDTA, and 7% w/v SDS. Probes were labeled with [α^{32}P] dCTP (New England Nuclear) using a High Prime labeling kit (Roche). Filters were rinsed once briefly, and then washed twice for 30 minutes at 65°C in washing solution I (20 mM Na phosphate buffer, pH 7.2, 1mM EDTA, 5% w/v SDS), and once at 65°C in washing solution II (20 mM Na phosphate buffer, pH 7.2, 1mM EDTA, 1% SDS w/v). The probe consisted of the plasmid pNTPΔ, which contains the same sequences as the integrated pNPT-tel plasmid, except that it does not contain telomeric repeat sequences.

2.8 Cloning and sequence analysis of the sites of chromosome healing and fusion

Analysis of sites of chromosome healing was performed using PCR with one primer complementary to the Puro^r gene (5′-GTGGGCTTGTACTCGGTCAT-3′) and one primer complementary to the telomeric repeat sequences (5′-AACCCTAACCCTAACCCTAACC-3′). PCR was performed as described previously [22] using an initial incubation for 2 min at 95°C, followed by 40 cycles of 95°C for 30 sec, 62°C for 30 sec, and 72°C for 30 sec, followed by one cycle of 95°C for 30 sec, 62°C for 30 sec, and 72°C for 2 min. Following their purification using a Qiaex II kit (Qiagen, Valencia, CA), the PCR products were sequenced directly by Molecular Cloning Laboratories (South San Francisco, CA), using the primer complementary to the Puro^r gene.

The cloning of the inverted repeats resulting from sister chromatid fusion was achieved by plasmid rescue. Plasmid rescue was performed by first digesting the DNA with XbaI, followed by the circularization and concentration of the DNA as described previously [23]. The DNA was then used to transform STBL2 chemically competent bacteria (Gibco), and the circularized plasmid and adjacent cellular DNA was selected using ampicillin. The rescued sequences were then mapped using restriction enzymes and sequenced from various primers specific for plasmid and puromycin resistance gene sequences.

2.9 Statistical analysis

Table 2 illustrates the number of events (healing, fusion, or loss) observed for each clone isolated from wild-type cells, or cells harboring a homozygous *PIF1* deletion or Nbs1 hypomorphism. Within and between each genotype, the likelihood that the frequency of each respective event differed from each other was assessed using ANOVA (Fisher's exact test, two-sided) using the software program Instat 3 (contained within Prism 5.0, www.graphpad.com). In cases where a significant difference was predicted by Fisher's exact test, a free software program called G-power 3 was used to calculate the alpha value of the comparison given the sample size and proportional effect observed (see Table 2 legend) (insert reference: Erdfelder, E., Faul, F., & Buchner, A. (1996). GPOWER: A general power analysis program. *Behavior Research Methods, Instruments, & Computers, 28*, 1–11) (Program can be downloaded from http://www.psycho.uni-duesseldorf.de/abteilungen/aap/gpower3/). A similar analysis was conducted for the data in Table 3; no statistical difference was observed in the incidence of events observed between PIF1+/+ and PIF1−/− clones.

3. Results

3.1 The generation of murine ES cell lines containing the telomeric pPPT2-tel plasmid

The murine ES cell lines used in this study all contain the pPPT2-tel plasmid located at the telomere on the long arm of chromosome 11. The pPPT2-tel plasmid is used to monitor the

consequences of DSBs near telomeres [21], and contains a gene whose expression confers puromycin resistance (Puro^r), an HSV-tk gene for negative selection with ganciclovir, and a recognition site for the I-SceI endonuclease used for the introduction of DSBs. The murine ES cells used in these studies were generated by crossing the 10P mouse with mice that were heterozygous for a *PIF1* deletion [24] or a *NBS1*$^{\Delta B}$ hypomorphic mutation [28]. PCR was then used to identify ES cell lines that were wild type, homozygous for a *PIF1* deletion (Figure S1), or homozygous for the *NBS1*$^{\Delta B}$ hypomorphic mutation (see Materials and Methods).

Similar to results reported during the initial generation and characterization of mice homozygous for the *PIF1* deletion [24], real-time quantitative PCR demonstrated no detectable *PIF1* transcripts in *PIF1* knockout ES cell lines (Table 1). Our RNA analysis also showed that *PIF1* is expressed at very low levels in wild type murine ES cells, as has been previously reported for both murine ES cells and a variety of human tissues [24, 25]. The level of expression of *PIF1* in our wild type cell lines is 0.02 to 0.04% of the level of expression of the highly expressed mitochondrial ribosomal protein L19, while expression of PIF1 is 0.01% to 0.03% of the level of expression of L19 in the cell lines heterozygous for the PIF1 knockout. This low level of Pif1 expression in murine ES cells is also reflected in the low level of protein that is detected by western blot analysis using PIF1-specific antibodies [24].

3.2 Method of monitoring the consequences of DSBs near telomeres in murine ES cells

The generation of DSBs near the telomere in the ES cell lines was accomplished by transient transfection with the pCBASce expression vector containing the I-SceI gene. Following transfection, the cells were replated the following day in medium containing ganciclovir to select for ganciclovir-resistant (Gan^r) subclones that had lost the HSV-tk gene. After 10 days, individual colonies were picked, expanded in culture, and the genomic DNA isolated. Southern blot analysis following digestion of genomic DNA with the XbaI restriction enzyme demonstrated that the Gan^r subclones fall into four categories (Figure 1). In the first category, some subclones lost the original 3.0 and 4.5 kbp bands and instead show a band at the top of the gel at the limit of resolution. As shown previously, nearly all of these subclones have undergone chromosome healing, which involves the addition of telomeric repeat sequences at or very near the I-SceI site [21, 22]. As in these earlier studies, chromosome healing was confirmed by PCR, using one primer complementary to the plasmid sequences proximal to the I-SceI site, and one primer complementary to the telomeric repeat sequences (data not shown). In the second category, some subclones lost the original bands and gained a new band (or bands) that varied in size in the different subclones. These subclones underwent telomere loss and gross chromosome rearrangements (GCRs) within the integrated plasmid sequences. The rescue of the rearranged plasmid sequences from five murine ES cell subclones containing I-SceI-induced GCRs showed that all five subclones contained inverted repeats [21, 23], which result from sister chromatid fusions as demonstrated previously [23, 38]. In the third category, some subclones show no change in the 3.0 and 4.3 kbp bands found in the parental 10P cell lines. These subclones underwent either point mutations or silencing of the HSV-tk gene due to the telomere position effect, as described previously [31, 32]. Finally, some subclones exhibited no plasmid-specific bands, and thus underwent a complete loss of the telomeric plasmid sequences likely due to degradation. We have shown previously that degradation occurs prior to most sister chromatid fusions, with deletions of up to 25 kbp that eliminate the plasmid sequences on one of the sister chromatids [21]. Therefore, the only difference between the subclones with rearranged plasmids and those that have completely lost the plasmid sequences is likely to be the extent of degradation at the DSB prior to the formation of GCRs.

3.3 The consequences of DSBs near telomeres in wild type murine ES cells

The results from the four independent wild type ES cell lines, 10PWT-FA, 10PWT-CP, 10PWT-FB, 10PWT-BA, demonstrated that the percentage of cells with chromosome healing at DSBs near a telomere was similar in all four wild type cell lines, accounting for 29 to 38% of the rearrangements detected by Southern blot analysis (Table 2). The remaining events involved either detectable GCRs or the complete loss of the plasmid sequences. Unlike chromosome healing, which was not significantly different in the four ES cell lines, the percentage of cells with GCRs and complete loss of the plasmid sequences was somewhat variable, with the CP cell line demonstrating significantly fewer GCRs than the other three wild type ES cell lines (Table 2). As discussed above, this variability in the percentage of cells with GCRs or loss of the plasmid is likely to reflect differences in the extent of degradation, because GCRs are commonly associated with extensive degradation. Consistent with this conclusion, the combined levels of complete plasmid loss and GCRs did not differ significantly for the four wild type ES cell lines (Table 2). Power value analysis confirmed that sample sizes within and between all groups exceeded the minimum required to determine statistical significance. In summary, the extent of degradation at DSBs near telomeres did not affect the efficiency of chromosome healing, which did not differ significantly in the four wild type ES cell lines.

3.4 The effect of Pif1 absence on chromosome healing and GCRs

The analysis of two independently isolated *Pif1* knockout ES cell clones, PIF-2H and PIF-9A, revealed that the percentage of cells with chromosome healing at DSBs near a telomere did not differ significantly from wild type ES cell lines (Table 2). Although this method cannot rule out small changes in the percentage of cells demonstrating chromosome healing, it is clear that PIF1 deficiency in mammalian cells does not have a dramatic effect on chromosome healing, as it does in *S. cerevisiae* [5, 6]. Mammalian PIF1 binds to TERT, however *Pif1* knockout mice appear normal and do not display abnormal telomere integrity or length [24, 25]. This functional redundancy or potential dispensability of Pif1 function in mice is consistent with our observation that *Pif1* deficiency does not promote the *de novo* addition of telomeric repeat sequences at DSBs near telomeres. However, this result does not rule out the possibility that *Pif1* may be involved in the inhibition of chromosome healing at DSBs at interstitial sites, where chromosome healing rarely occurs.

The percentage of cells demonstrating GCRs was significantly lower in the *Pif1* knockout ES cell lines than in three wild type ES cell lines (FA, FB and BA), but did not differ significantly from the fourth wild type ES cell line (CP) (Table 2). In addition, there was no significant difference between *Pif1* knockout clones and wild-type clones when plasmid loss and GCRs were combined together (Table 2). Therefore, the low level of GCRs in the *Pif1* knockout ES cell lines may not be significant.

3.5 The effect of the Nbs1$^{\Delta B}$ hypomorph on chromosome healing and GCRs

Studies in *S. cerevisiae* demonstrated that the MRX complex is required for chromosome healing [8], while a deficiency in the resection of DSBs and the activation of the Mec1-mediated cell cycle checkpoint promotes chromosome healing [10, 11]. We investigated the importance of the MRN complex in mammalian DSB processing near telomeres on chromosome healing using murine ES cell lines homozygous for the *Nbs1*$^{\Delta B}$ hypomorphic mutation. *Nbs1*$^{\Delta B/\Delta B}$ cells are sensitive to ionizing radiation [28], consistent with the role of the MRN complex in the processing of DSBs [39] and in regulating the activity of Atm in response to DSBs [40]. Two independently isolated *Nbs1*$^{\Delta B/\Delta B}$ ES cell clones, NBS-7C and NBS-8H, exhibited no significant difference compared with wild-type cells in their ability perform chromosome healing as a result of DSBs near telomeres, whether comparing total events within each genotype or each clone considered separately (Table 2). Therefore,

although we cannot rule out small changes in the percentage of cells demonstrating chromosome healing, a deficiency in the MRX complex in mammalian cells does not prevent chromosome healing as it does in *S. cerevisiae* [8].

As observed with chromosome healing, *Nbs1*$^{\Delta B/\Delta B}$ also had no significant effect on the frequency of large deletions and GCRs as a result of I-SceI-induced DSBs near telomeres when compared with WT clones (Table 2). Our earlier studies demonstrated that the GCRs resulting from DSBs near telomeres primarily involve large inverted repeats resulting from sister chromatid fusions. To confirm whether the GCRs in the Gan^r subclones of the *Nbs1*$^{\Delta B/\Delta B}$ ES cell lines consisted of sister chromatid fusions, the rearranged pPPT2-tel plasmid sequences were rescued from two of the subclones, NBS-7C-P3 and NBS-7C-P7 that were selected with ganciclovir and puromycin following the induction of DSBs. Selection with puromycin was included to insure that the Puro^r gene was conserved in at least one of the plasmids involved in the formation of the inverted repeat. Consistent with our earlier results [21, 23], the rescued plasmid sequences from both NBS-7C-P3 and NBS-7C-P7 contained inverted repeats (data not shown). The rescued plasmid from subclone NBS-7C-P3 contained a nearly perfect inverted repeat that occurred within 100 bp of the I-SceI site. The rescued plasmid from subclone NBS-7C-P7 also contained an inverted repeat, one end of which occurred within 14 bp of the I-SceI site, while the other end was located 1.2 kbp from the Puro^r polyA sequence. Thus, one sister chromatid underwent very little degradation, while the other sister chromatid underwent 1.2 kbp of degradation prior to fusion. The analysis of the rescued plasmid sequences demonstrates that, as in wild-type murine ES cells, sister chromatid fusions are the most common type of GCR resulting from DSBs near telomeres in NBS1$^{\Delta B/\Delta B}$ ES cell lines.

3.6 Comparison of sites of chromosome healing in wild type and PIF1 knockout cell lines

We demonstrated previously that chromosome healing near telomeres in mammalian cells almost always occurs at the site of an I-SceI-induced DSB without degradation [21, 22]. In yeast, chromosome healing usually occurs near telomeric repeat sequences [11, 41]. However, in yeast deficient in *PIF1*, telomere addition occurs at random locations following more extensive degradation than wild type cells [5, 6]. To determine whether *Pif1* knockout affects the extent of degradation prior to chromosome healing in mammalian cells, we compared the sites of chromosome healing in the I-SceI-induced Gan^r subclones generated from wild type and *Pif1* knockout ES cell lines (Table 3). As in wild type cells, chromosome healing in *Pif1* knockout ES cell lines occurred primarily at sites of microhomology at the I-SceI-induced DSB with little or no degradation. The percentage of chromosome healing at site A, the last nucleotide of the 4 nt overhang, or site B, the 5 nt immediately adjacent to the 4 nt overhang, were 54.5% and 32.7% for wild type ES cells, and 47.3% and 30.9% for *Pif1* knockout ES cells, respectively. Statistical analysis (using Fisher's exact test, see Methods) revealed no significant difference in these frequencies between wild type and *Pif1* knockout ES cells. In both cell types, there were a small number of Gan^r subclones that underwent chromosome healing at site C, involving 2 nt of homology in the 4 nt overhang, or that involved point mutations during chromosome healing at the I-SceI site. Only one of the 55 wild type Gan^r subclones that were analyzed (10PWT-FA-13) underwent chromosome healing at a site that was not located at the I-SceI-induced DSB, occurring after 25 bp of degradation (Figure 2). Four of the 55 PIF1 knockout Gan^r subclones that were analyzed underwent chromosome healing at sites that were not located at the I-SceI-induced DSB. The extent of degradation in two of these PIF1 knockout subclones was 71 bp for subclone PIF-2H-22, and 197 bp for subclone PIF-9D-26. A third subclone, PIF-9A-3, contained a mixture of cells with two different sites of chromosome healing, one that involved the degradation of 98 bp, and one that involved the degradation of 123 bp.

Chromosome healing in this subclone therefore occurred on two separate occasions, both following degradation of the DSB. In view of their close proximity, it is highly likely that both chromosome-healing events originated from the same initial DSB, but how this event may have occurred is unknown. Chromosome healing in a fourth I-SceI-induced Gan^r subclone isolated from one PIF1 knockout ES cell clone, PIF-9D-41, contained a 65 bp inverted fragment of chromosome 11 that was originally found 1275 bp proximal to the pPPT2-tel plasmid (Figure 2). The recombination junction between the plasmid and chromosome 11 sequences contained 3 bp of microhomology. This inverted repeat of the end of chromosome 11 is typical of sister chromatid fusions observed as a result of DSBs near telomeres, which can involve the degradation of one sister chromatid to a larger extent than the other [21, 23].

The combined results of the DNA sequence analysis demonstrated that the frequency of chromosome healing at sites other than the initial DSB was slightly greater in the *Pif1* knockout ES cell lines (4 of 55) than in the wild type ES cell lines (1 of 55). However, this difference was not significant (p=0.36, Fisher's exact test), and the great majority of events occurred at the I-SceI-site in both the wild type and *Pif1* knockout ES cell lines. In addition, these results suggest that *Pif1* disruption did not affect the limited microhomology used by telomerase to initiate *de novo* telomere addition [15, 16].

4. Discussion

The generation of DSBs with I-SceI endonuclease enabled us to test, for the first time in mammals, the importance of Pif1 in the regulation of chromosome healing at DSBs near telomeres. Although the sensitivity of our assay system does not allow us to rule out the possibility of small differences in chromosome healing, it is clear from our studies that a deficiency in PIF1 has minimal consequences for chromosome healing compared to S. cerevisiae. Mammalian PIF1 binds to TERT [24, 25], however, the prevalence of chromosome healing at DSBs near telomeres in murine ES cells demonstrates that Pif1 does not prevent *de novo* telomere addition at DSBs near telomeres. The absence of a detectable increase in chromosome healing in murine ES cells deficient in *Pif1* may imply that the regulation of chromosome healing is redundant in mammalian cells. This conclusion is consistent with the lack of chromosome instability and sensitivity to ionizing radiation observed in *Pif1* knockout mice, and the fact that telomere length remained unaltered compared with wild-type mice [24]. Had *Pif1* dramatically affected chromosome healing in murine cells, one would have predicated an increase in the level of chromosome instability and sensitivity to ionizing radiation, because it would be predicted to interfere with DSB repair and increase the frequency of terminal deletions.

In addition to redundancy, it is also possible that the regulation of chromosome healing may be different at telomeric and interstitial DSBs. Although chromosome healing is a common event near telomeres in murine ES cells, chromosome healing has not been observed at interstitial DSBs in mammalian cells [17–19]. Chromosome healing therefore appears to be suppressed at DSBs occurring at most locations, possibly to prevent it from interfering with DSB repair, as has been proposed in yeast [4]. This difference in the frequency of chromosome healing at telomeric and interstitial sites has led us to propose that chromosome healing serves an important function to compensate for the sensitivity of subtelomeric regions to DSBs [42–44]. This hypothesis is based on our demonstration that chromosome healing prevents the extensive degradation and chromosome instability that commonly results from DSBs near telomeres [42, 44]. The difference in chromosome healing at telomeric and interstitial sites could also be a result of a difference in regulation of Pif1 at these locations. In yeast, the inhibition of chromosome healing by Pif1 requires the phosphorylation of Pif1 by Mec1 in response to DSBs [45]. This inactivation of PIF1 may

be inhibited near telomeres in mammalian cells, because the telomeric protein TRF2 inhibits the mammalian homolog of MEC1, ATM [46].

The percentage of cells that exhibited GCRs in *Pif1* knockout ES cells was significantly lower than three of four wild type ES cell lines. However, chromosome healing in the *Pif1* knockout ES cell lines did not differ significantly from the chromosome healing in one wild type ES cell line. Pif1 does not therefore appear to have a significant influence on GCRs, whether via an influence upon chromosome healing, DNA resection or degradation. Because Pif1 is also involved in the resection of chromosome ends following telomere loss in yeast [47], the requirement for mammalian PIF1 may differ from yeast Pif1 in both chromosome healing and DNA resection.

An interesting observation made in the course of our studies is the presence of an inverted repeat located between the I-SceI-induced DSB and the site of telomere addition in subclone PIF-9D-41 (Figure 2). This inverted repeat is similar to the rearrangements found in subclones undergoing breakage/fusion/bridge (B/F/B) cycles, which we have shown previously result from sister chromatid fusions [21, 23, 44]. Once initiated, B/F/B cycles can continue for many generations until the chromosome acquires a new telomere, which restores chromosome stability. Telomere acquisition most often occurs by translocation of the end of another chromosome in both murine ES cells [23] and human tumor cell lines [48]. Unlike DSBs near telomeres, chromosome healing is a relatively rare event during B/F/B cycles, possibly because these breaks do not occur near telomeres. However, the presence of an inverted repeat proximal to the site of chromosome healing in subclone PIF-9A-41 suggests that chromosome healing stabilized this chromosome after it had initiated B/F/B cycles. The break site in subclone PIF-9A-41 would have occurred very near the site of fusion, which is not unlikely, since previous data suggests that fused sister chromatids usually break within 1 Mbp of the site of fusion [38]. Chromosome healing following breakage of sister chromatids in subclone PIF-9A-41 therefore would have occurred at an interstitial site far from a telomere. Whether the addition of a telomere at an interstitial site in this particular instance was a result of *Pif1* deficiency cannot be determined. Regardless, the ability of chromosome healing to end B/F/B cycles has important implications for limiting the chromosome instability resulting from telomere loss.

The percentage of cells that exhibited chromosome healing near telomeres in the $Nbs1^{\Delta B/\Delta B}$ ES cell lines did not differ significantly from wild type ES cell lines. Therefore, any influence of the $Nbs1^{\Delta}$ hybpmorph on chromosome healing, if any, must be relatively small. The $Nbs1^{\Delta B}$ hypomorphic allele contains a deletion of exons 4 and 5 [28], which contain the FHA domain that is critical for the processing of DSBs [26, 27]. The FHA region of Nbs1 is required for tethering CtIP [26], which facilitates the transition from DSB sensing to processing [49, 50]. The failure of the $Nbs1^{\Delta B}$ hypomorph to affect the frequency of chromosome healing is somewhat surprising in view of the requirement of the MRX complex for healing of a telomeric DSB induced during nocodazole arrest in *S. cerevisiae* [8]. This role of the MRX complex in chromosome healing in *S. cerevisiae* was proposed to be due to the requirement of processing of the DSB for recruitment of telomerase. However, the processing of DSBs does not appear to be necessary for chromosome healing in murine ES cells, because the $Nbs1^{\Delta B}$ hypomorph lacks the FHA domain required for recruitment of CtIP, a critical protein involved in the processing of DSBs [26, 27].

Our results also suggest that Nbs1 is not required to generate the large deletions and GCRs that occurred in response to DSBs near telomeres. Although small differences in large deletions and GCRs cannot be ruled out, our results indicate that the $Nbs1^{\Delta B}$ hypomorph does not have a dramatic effect on either repair or degradation at DSBs near telomeres. At first glance, this finding would appear to conflict with the results demonstrating a

requirement for Mre11 and Nbs1 in GCRs resulting from loss of telomere function. A study by Attwooll *et al.* found that the Nbs1$^{\Delta B}$ hypomorph decreased the frequency of chromosome fusions resulting from telomere shortening in *Tert* knockout cells [51]. In addition, they found that an Mre11 hypomorph decreased the frequency of chromosome fusions in *Tert* knockout cells [51]. Similarly, Deng *et al.* [52] found that knockdown of CtIP decreased the frequency chromosome fusions in Trf2-depleted cells that were also deficient in both *Tpp1* and *53BP1*, and were therefore unable to fuse chromosomes by C-NHEJ [53]. These results suggest that dysfunctional telomeres must be processed prior to chromosome fusion by A-NHEJ. However, the processing of the ends of dysfunctional telomeres and V(D)J recombination is likely to proceed via a different mechanism than the processing of subtelomeric I-SceI-induced DSBs in our studies. Although a deficiency in Mre11 can inhibit the repair of I-SceI-induced DSBs by both C-NHEJ and A-NHEJ [54, 55], knockdown of Nbs1 inhibited the repair of DSBs by C-NHEJ, but not A-NHEJ [55]. Moreover, the knockdown of CtIP did not limit the extent of degradation during repair of I-SceI-induced DSBs in cells deficient in C-NHEJ, whereas knockdown of Mre11 did limit degradation [55]. Therefore, consistent with our results, the Nbs1$^{\Delta B}$ hypomorph would not influence chromosome fusion in response to DSBs near telomeres if these DSBs were repaired by A-NHEJ. Although the Nbs1$^{\Delta B}$ hypomorph inhibited the A-NHEJ of signal ends during V(D)J recombination, this effect was proposed to be due to the inability to process the hairpins at the DNA ends [56], which would not be a necessary step during the repair of I-SceI-induced DSBs. The prevalence of repair of DSBs near telomeres by A-NHEJ would be consistent with the increased frequency of large deletions and GCRs previously reported as a result of DSBs near telomeres, when compared to other locations [42, 44], since A-NHEJ is associated with large deletions and GCRs [57–59]. In summary, our results provide compelling genetic evidence that multiple pathways have evolved in response to a telomere-proximal DSB in mammals, and that neither Pif1 nor Nbs1 alone are solely responsible for chromosome healing in this setting.

Supplementary Material

Refer to Web version on PubMed Central for supplementary material.

Acknowledgments

This work was supported by the National Institute of Environmental Health Science [grant number RO1 ES008427] to [J.M.]; and a Stewart Trust Cancer Research Award from the UCSF Helen Diller Family Comprehensive Cancer to [J.M.]; and the National Institutes of Health, National Institute on Aging [grant number RO1 AG02398] to [L.A.H.].

Abbreviations

A-NHEJ	Alternative nonhomologous end joining
B/F/B	Breakage/Fusion/Bridge
C-NHEJ	Classical nonhomologus end joining
DSBs	Double-strand breaks
ES	Embryonic stem
Gan^{r}	Ganciclovir-resistant
GCRs	Gross chromosome rearrangements
HSV-tk	Herpes simplex virus thymidine kinase

PGK	3-phosphoglycerate kinase
PCR	Polymerase chain reaction
rt-PCR	Real time quantitative PCR

References

1. Blackburn EH, Greider CW, Szostak JW. Telomeres and telomerase: the path from maize, Tetrahymena and yeast to human cancer and aging. Nat Med. 2006; 12:1133–1138. [PubMed: 17024208]
2. Artandi SE, DePinho RA. Telomeres and telomerase in cancer. Carcinogenesis. 2010; 31:9–18. [PubMed: 19887512]
3. Diede SJ, Gottschling DE. Telomerase-mediated telomere addition in vivo requires DNA primase and DNA polymerase α and δ. Cell. 1999; 99:723–733. [PubMed: 10619426]
4. Zhou JQ, Monson EK, Teng SC, Schultz VP, Zakian VA. Pif1p helicase, a catalytic inhibitor of telomerase in yeast. Science. 2000; 289:771–774. [PubMed: 10926538]
5. Schulz VP, Zakian VA. The Saccharomyces *PIF1* DNA helicase inhibits telomere elongation and de novo telomere formation. Cell. 1994; 76:145–155. [PubMed: 8287473]
6. Pennaneach V, Putnam CD, Kolodner RD. Chromosome healing by de novo telomere addition in Saccharomyces cerevisiae. Mol Microbiol. 2006; 59:1357–1368. [PubMed: 16468981]
7. Eugster A, Lanzuolo C, Bonneton M, Luciano P, Pollice A, Pulitzer JF, Stegberg E, Berthiau AS, Forstemann K, Corda Y, Lingner J, Geli V, Gilson E. The finger subdomain of yeast telomerase cooperates with Pif1p to limit telomere elongation. Nat Struct Mol Biol. 2006; 13:734–739. [PubMed: 16878131]
8. Diede SJ, Gottschling DE. Exonuclease activity is required for sequence addition and Cdc13p loading at a de novo telomere. Curr Biol. 2001; 11:1336–1340. [PubMed: 11553326]
9. Goudsouzian LK, Tuzon CT, Zakian VA. S. cerevisiae Tel1p and Mre11p are required for normal levels of Est1p and Est2p telomere association. Mol Cell. 2006; 24:603–610. [PubMed: 17188035]
10. Chung WH, Zhu Z, Papusha A, Malkova A, Ira G. Defective resection at DNA double-strand breaks leads to de novo telomere formation and enhances gene targeting. PLoS Genet. 2010; 6:e1000948. [PubMed: 20485519]
11. Lydeard JR, Lipkin-Moore Z, Jain S, Eapen VV, Haber JE. Sgs1 and exo1 redundantly inhibit break-induced replication and De Novo telomere addition at broken chromosome ends. PLoS Genet. 2010; 6:e1000973. [PubMed: 20523895]
12. Varley H, Di S, Scherer SW, Royle NJ. Characterization of terminal deletions at 7q32 and 22q13.3 healed by de novo telomere addition. Am J Hum Genet. 2000; 67:610–622. [PubMed: 10924407]
13. Wong AC, Ning Y, Flint J, Clark K, Dumanski JP, Ledbetter DH, McDermid HE. Molecular characterization of a 130-kb terminal microdeletion at 22q in a child with mild mental retardation. Am J Hum Genet. 1997; 60:113–120. [PubMed: 8981954]
14. Flint J, Thomas K, Micklem G, Raynham H, Clark K, Doggett NA, King A, Higgs DR. The relationship between chromosome structure and function at a human telomeric region. Nat Genet. 1997; 15:252–257. [PubMed: 9054936]
15. Morin GB. Recognition of a chromosome truncation site associated with α-thalassaimia by human telomerase. Nature. 1991; 353:454–456. [PubMed: 1896089]
16. Harrington LA, Greider CW. Telomerase primer specificity and chromosome healing. Nature. 1991; 353:451–454. [PubMed: 1896088]
17. Honma M, Sakuraba M, Koizumi T, Takashima Y, Sakamoto H, Hayashi M. Non-homologous end-joining for repairing I-SceI-induced DNA double strand breaks in human cells. DNA Repair (Amst). 2007; 6:781–788. [PubMed: 17296333]
18. Lin Y, Waldman AS. Capture of DNA sequences at double-strand breaks in mammalian cells. Genetics. 2001; 158:1665–1674. [PubMed: 11514454]

19. Rebuzzini P, Khoriauli L, Azzalin CM, Magnani E, Mondello C, Giulotto E. New mammalian cellular systems to study mutations introduced at the break site by non-homologous end-joining. DNA Repair (Amst). 2005; 4:546–555. [PubMed: 15811627]
20. Latre L, Genesca A, Martin M, Ribas M, Egozcue J, Blasco MA, Tusell L. Repair of DNA broken ends is similar in embryonic fibroblasts with and without telomerase. Radiat Res. 2004; 162:136–142. [PubMed: 15387140]
21. Gao Q, Reynolds GE, Wilcox A, Miller D, Cheung P, Artandi SE, Murnane JP. Telomerase-dependent and -independent chromosome healing in mouse embryonic stem cells. DNA Repair. 2008; 7:1233–1249. [PubMed: 18502190]
22. Sprung CN, Reynolds GE, Jasin M, Murnane JP. Chromosome healing in mouse embryonic stem cells. Proc Natl Acad Sci USA. 1999; 96:6781–6786. [PubMed: 10359789]
23. Lo AWI, Sprung CN, Fouladi B, Pedram M, Sabatier L, Ricoul M, Reynolds GE, Murnane JP. Chromosome instability as a result of double-strand breaks near telomeres in mouse embryonic stem cells. Mol Cell Biol. 2002; 22:4836–4850. [PubMed: 12052890]
24. Snow BE, Mateyak M, Paderova J, Wakeham A, Iorio C, Zakian V, Squire J, Harrington L. Murine Pif1 interacts with telomerase and is dispensable for telomere function in vivo. Mol Cell Biol. 2007; 27:1017–1026. [PubMed: 17130244]
25. Mateyak MK, Zakian VA. Human PIF helicase is cell cycle regulated and associates with telomerase. Cell Cycle. 2006; 5:2796–2804. [PubMed: 17172855]
26. Williams RS, Dodson GE, Limbo O, Yamada Y, Williams JS, Guenther G, Classen S, Glover JN, Iwasaki H, Russell P, Tainer JA. Nbs1 flexibly tethers Ctp1 and Mre11-Rad50 to coordinate DNA double-strand break processing and repair. Cell. 2009; 139:87–99. [PubMed: 19804755]
27. Lloyd J, Chapman JR, Clapperton JA, Haire LF, Hartsuiker E, Li J, Carr AM, Jackson SP, Smerdon SJ. A supramodular FHA/BRCT-repeat architecture mediates Nbs1 adaptor function in response to DNA damage. Cell. 2009; 139:100–111. [PubMed: 19804756]
28. Williams BR, Mirzoeva OK, Morgan WF, Lin J, Dunnick W, Petrini JHJ. A murine model of Nijmegen Breakage Syndrome. Curr Biol. 2002; 12:648–653. [PubMed: 11967151]
29. Stracker TH, Couto SS, Cordon-Cardo C, Matos T, Petrini JH. Chk2 suppresses the oncogenic potential of DNA replication-associated DNA damage. Mol Cell. 2008; 31:21–32. [PubMed: 18614044]
30. Shull ER, Lee Y, Nakane H, Stracker TH, Zhao J, Russell HR, Petrini JH, McKinnon PJ. Differential DNA damage signaling accounts for distinct neural apoptotic responses in ATLD and NBS. Genes Dev. 2009; 23:171–180. [PubMed: 19171781]
31. Gao Q, Reynolds GE, Innes L, Pedram M, Jones E, Junabi M, Gao DW, Ricoule M, Sabatier L, Van Brocklin H, Franc BL, Murnane JP. Telomeric transgenes are silenced in adult mouse tissues and embryo fibroblasts, but are expressed in embryonic stem cells. Stem Cells. 2007; 25:3085–3092. [PubMed: 17823235]
32. Pedram M, Sprung CN, Gao Q, Lo AWI, Reynolds G, Murnane JP. Telomere position effect and silencing of transgenes near telomeres in the mouse. Mol Cell Biol. 2006; 26:1865–1878. [PubMed: 16479005]
33. Nagy, A.; Gertsenstein, M.; Vinersten, K.; Behringer, R. Manipulating the mouse embryo: a laboratory manual. 3. Cold Spring Harbor Laboratory Press; 2003.
34. Collins C, Rommens JM, Kowbel D, Godfrey T, Tanner M, Hwang SI, Polikoff D, Nonet G, Cochran J, Myambo K, Jay KE, Froula J, Cloutier T, Kou WL, Yaswen P, Dairkee S, Giovanola J, Hutchinson GB, Isola J, Kallioniemi OP, Palazzolo M, Martin C, Ericsson C, Pinkel D, Albertson D, Li WB, Gray JW. Positional cloning of ZNF217 and NABC1: Genes amplified at 20q13.2 and overexpressed in breast carcinoma. Proc Natl Acad Sci USA. 1998; 95:8703–8708. [PubMed: 9671742]
35. Richardson C, Moynahan ME, Jasin M. Double-strand break repair by interchromosomal recombination: suppression of chromosomal translocations. Genes Dev. 1998; 12:3831–3842. [PubMed: 9869637]
36. Brisebois JJ, DuBow MS. Selection for spontaneous null mutations in a chromosomally-integrated HSV-1 thymidine kinase gene yields deletions and a mutation caused by intragenic illegitimate recombination. Mutat Res. 1993; 287:191–205. [PubMed: 7685479]

37. Murata S, Matsuzaki T, Takai S, Yaoita H, Noda M. A new retroviral vector for detecting mutations and chromosomal instability in mammalian cells. Muatat Res. 1995; 334:375–383.
38. Lo AWI, Sabatier L, Fouladi B, Pottier G, Ricoul M, Murnane JP. DNA amplification by breakage/fusion/bridge cycles initiated by spontaneous telomere loss in a human cancer cell line. Neoplasia. 2002; 6:531–538. [PubMed: 12407447]
39. Zha S, Boboila C, Alt FW. Mre11: roles in DNA repair beyond homologous recombination. Nat Struct Mol Biol. 2009; 16:798–800. [PubMed: 19654615]
40. Lavin MF. ATM and the Mre11 complex combine to recognize and signal DNA double-strand breaks. Oncogene. 2007; 26:7749–7758. [PubMed: 18066087]
41. Kramer KM, Haber JE. New telomeres in yeast are initiated with a highly selected subset of $TG_{1–3}$ repeats. Genes Dev. 1993; 7:2345–2356. [PubMed: 8253381]
42. Kulkarni A, Zschenker O, Reynolds G, Miller D, Murnane JP. The effect of telomere proximity on telomere position effect, chromosome healing and sensitivity to DNA double-strand breaks in a human tumor cell line. Mol Cell Biol. 2010 in press.
43. Murnane JP. Telomere loss as a mechanism for chromosomal instability in human cancer. Cancer Res. 2010; 70:4255–4259. [PubMed: 20484032]
44. Zschenker O, Kulkarni A, Miller D, Reynolds GE, Granger-Locatelli M, Pottier G, Sabatier L, Murnane JP. Increased sensitivity of subtelomeric regions to DNA double-strand breaks in a human tumor cell line. DNA Repair. 2009; 8:886–900. [PubMed: 19540174]
45. Makovets S, Blackburn EH. DNA damage signalling prevents deleterious telomere addition at DNA breaks. Nat Cell Biol. 2009; 11:1383–1386. [PubMed: 19838171]
46. Karlseder J, Hoke K, Mirzoeva OK, Bakkenist C, Kastan MB, Petrini JH, de Lange T. The telomeric protein TRF2 binds the ATM kinase and can inhibit the ATM-dependent DNA damage response. PLoS Biol. 2004; 2:E240. [PubMed: 15314656]
47. Dewar JM, Lydall D. Pif1- and Exo1-dependent nucleases coordinate checkpoint activation following telomere uncapping. EMBO J. 2010; 29:4020–4034. [PubMed: 21045806]
48. Sabatier L, Ricoul M, Pottier G, Murnane JP. The loss of a single telomere can result in genomic instability involving multiple chromosomes in a human tumor cell line. Mol Cancer Res. 2005; 3:139–150. [PubMed: 15798094]
49. Sartori AA, Lukas C, Coates J, Mistrik M, Fu S, Bartek J, Baer R, Lukas J, Jackson SP. Human CtIP promotes DNA end resection. Nature. 2007; 450:509–514. [PubMed: 17965729]
50. You Z, Shi LZ, Zhu Q, Wu P, Zhang YW, Basilio A, Tonnu N, Verma IM, Berns MW, Hunter T. CtIP links DNA double-strand break sensing to resection. Mol Cell. 2009; 36:954–969. [PubMed: 20064462]
51. Attwooll CL, Akpinar M, Petrini JH. The mre11 complex and the response to dysfunctional telomeres. Mol Cell Biol. 2009; 29:5540–5551. [PubMed: 19667076]
52. Deng Y, Guo X, Ferguson DO, Chang S. Multiple roles for MRE11 at uncapped telomeres. Nature. 2009; 460:914–918. [PubMed: 19633651]
53. Rai R, Zheng H, He H, Luo Y, Multani A, Carpenter PB, Chang S. The function of classical and alternative non-homologous end-joining pathways in the fusion of dysfunctional telomeres. Embo J. 2010; 29:2598–2610. [PubMed: 20588252]
54. Rass E, Grabarz A, Plo I, Gautier J, Bertrand P, Lopez BS. Role of Mre11 in chromosomal nonhomologous end joining in mammalian cells. Nat Struct Mol Biol. 2009; 16:819–824. [PubMed: 19633668]
55. Xie A, Kwok A, Scully R. Role of mammalian Mre11 in classical and alternative nonhomologous end joining. Nat Struct Mol Biol. 2009; 16:814–818. [PubMed: 19633669]
56. Deriano L, Stracker TH, Baker A, Petrini JH, Roth DB. Roles for NBS1 in alternative nonhomologous end-joining of V(D)J recombination intermediates. Mol Cell. 2009; 34:13–25. [PubMed: 19362533]
57. Gao Y, Ferguson DO, Xie W, Manis JP, Sekiguchi J, Frank KM, Chaudhuri J, Horner J, DePinho RA, Alt FW. Interplay of p53 and DNA-repair protein XRCC4 in tumorigenesis, genomic instability and development. Nature. 2000; 404:897–900. [PubMed: 10786799]

58. Guirouilh-Barbat J, Huck S, Bertrand P, Pirzio L, Desmaze C, Sabatier L, Lopez BS. Impact of the KU80 pathway on NHEJ-induced genome rearrangements in mammalian cells. Mol Cell. 2004; 14:611–623. [PubMed: 15175156]

59. Weinstock DM, Brunet E, Jasin M. Formation of NHEJ-derived reciprocal chromosomal translocations does not require Ku70. Nat Cell Biol. 2007; 9:978–981. [PubMed: 17643113]

HIGHLIGHTS

A deficiency in PIF1 had no affect on chromosome healing at DSBs near telomeres in mouse ES cells, despite the fact that inactivation of PIF1 increases chromosome healing by 1000-fold in yeast. The regulation of chromosome healing in mammalian cells is therefore redundant or different from yeast.

Haploinsufficiency in NBS1 that affects the processing of DSBs had no affect on chromosome healing in mouse ES cells, despite the fact that a deficiency in the processing of DSBs stimulates chromosome healing in yeast. The factors influencing chromosome healing in mammalian cells are different from those in yeast.

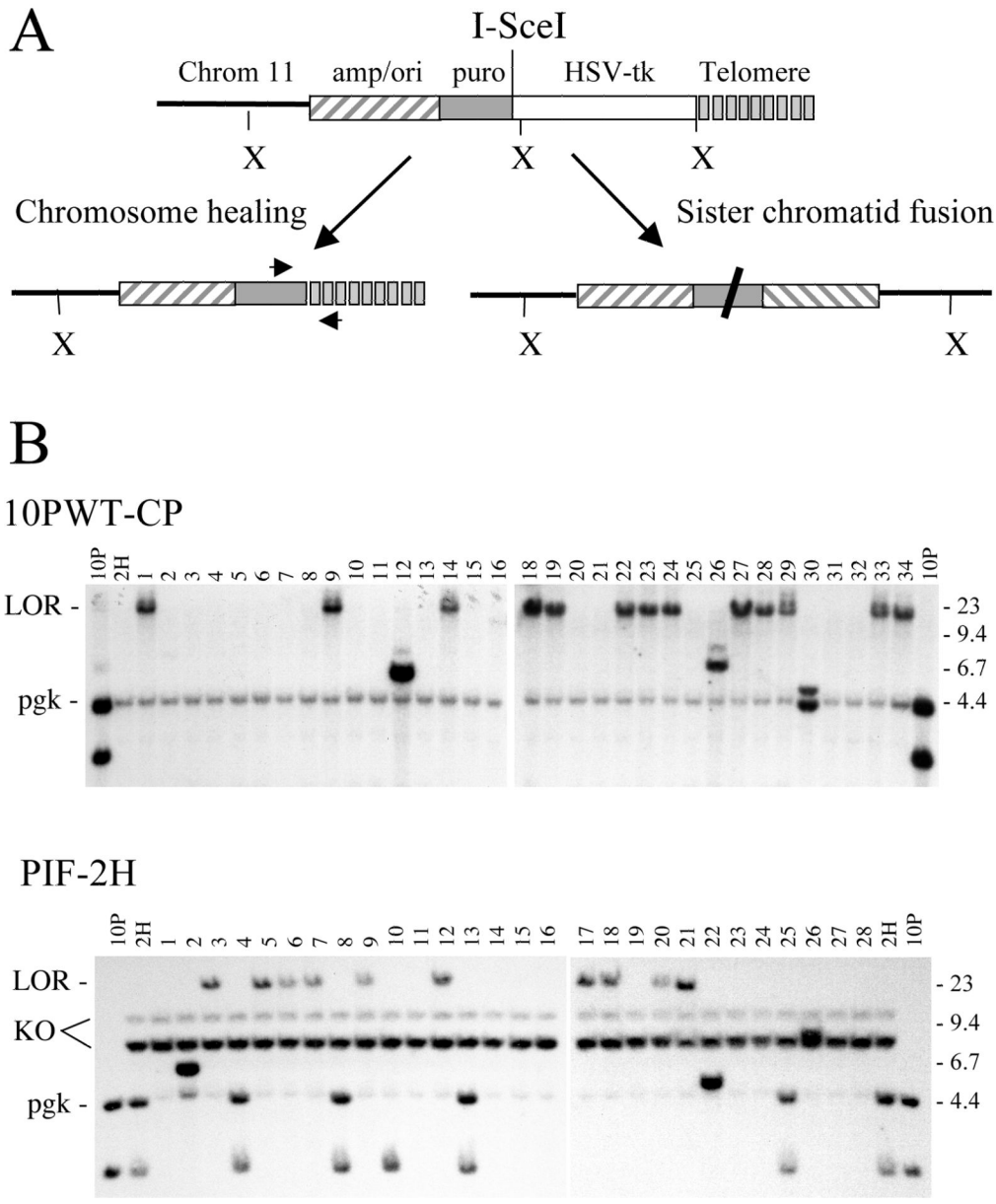

Fig. 1.

Analysis of rearrangements resulting from a DSB near a telomere in wild type or *Pif1* knockout ES cell lines. (A) The structure of the telomeric pPPT2-tel plasmid sequences and the types of rearrangements resulting from I-*Sce*I-induced DSBs in murine ES cell lines used in this study. The pPPT2-tel plasmid in ES cell clone 10P seeded the formation of a new telomere upon integration 1.4 Mbp from the end of chromosome 11. The telomere contains an ampicillin-resistance gene and plasmid origin of replication (amp/ori), a puromycin-resistance gene (Puro), an HSV-tk gene, an I-SceI endonuclease recognition site, and telomeric repeat sequences (telomere). The locations of the XbaI restriction sites used for Southern blot analysis are also shown. I-SceI endonuclease-induced DSBs near the telomere result in chromosome healing involving the addition of telomeric repeat sequences at the site of the break (lower left), inverted repeats resulting from sister chromatid fusion (lower right), or complete loss of the plasmid sequences (not shown). PCR using primers specific

for the Puro^r gene and telomeric repeat sequences (arrows) and DNA sequence analysis are used to confirm the presence of a new telomere at the I-SceI site. (B) Southern blot analysis was performed on genomic DNA from I-*Sce*I-induced Gan^r subclones of the wild type 10PWT-CP and *Pif1* knockout PIF-2H ES cell lines. DNA was digested with XbaI and hybridization was performed using the pNPTΔ plasmid as a probe (with no telomeric repeat sequences). Molecular weight markers consisting of Lambda bacteriophage HindIII fragments, as indicated. The unrearranged telomeric plasmid sequences in the parental wild type 10PWT-CP (10P) and *Pif1* knockout PIF-2H (2H) ES cell lines produce two plasmid-specific bands, a 3 kbp band containing the HSV-tk gene, and a 4.3 kbp band containing the internal portion of the plasmid and adjacent cellular DNA (see Figure S1). In contrast, the I-SceI-induced Gan^r subclones demonstrated a large XbaI plasmid-specific band at the limit of resolution (LOR) as a result of chromosome healing, variable-sized bands containing inverted repeats, or no plasmid-specific bands due to complete loss of the plasmid sequences. The hybridization of the murine *Pgk* gene promoter and polyA addition sequences in the pNPTΔ plasmid probe to the endogenous murine *Pgk* gene results in a light band of 4.4 kbp (pgk), while the plasmid sequences used to disrupt the *Pif1* gene result in two bands of 8 and 10 kbp (KO).

Wild type

```
pPPT-tel       TTGCTTCCTCTTGAAAACCACACTGCGCGACTCTAGTAGGGATA
               *************** *     *  *           **
Clone FA-13    TTGCTTCCTCTTGAAATCAGGGTTAGGGTTAGGGTTAGGGTTAG
                 * **    **    * *************************
Tel repeats    AGGGTTAGGGTTAGGGTTAGGGTTAGGGTTAGGGTTAGGGTTAG
```

25 bp deletion, mutation at telomere addition site

PIF1 knockout

```
pPPT-tel       CACACTGCTCGACATTGGGTGGAAACATTCCAGGCCTGGGTGGA
               ******************   *    *         *   **
Clone 2H-22    CACACTGCTCGACATTGGGATTAGGGTTAGGGTTAGGGTTAGGG
                     * *     ** ** ************************
Tel repeats    GGTTAGGGTTAGGGTTAGGGTTAGGGTTAGGGTTAGGGTTAGGG
```

71 bp deletion, mutation at telomere addition site

```
pPPT-tel       CGACTGCATCTGCGTGTTCGAATTCGCCAATGACAAGACGCTGG
               ****************** *  ** **    *       *   *
Clone 9D-26    CGACTGCATCTGCGTGTTAGGGTTAGGGTTAGGGTTAGGGTTAG
                   *     *  * ****************************
Tel repeats    AGGGTTAGGGTTAGGGTTAGGGTTAGGGTTAGGGTTAGGGTTAG
```

197 bp deletion, 3 bp homology at addition site

```
pPPT-tel       GAAACATTCCAGGCCTGGGTGGAGAGGCTTTTTGCTTCCTCTTG
               ****************** *   *      ** *  *     *
Clone 9A-3     GAAACATTCCAGGCCTGGTTAGGGTTAGGGTTAGGGTTAGGGTT
               ******************************************
Tel repeats    TTAGGGTTAGGGTTAGGGTTAGGGTTAGGGTTAGGGTTAGGGTT
```

98 bp deletion, 2 bp homology at addition site

```
pPPT-tel       GGCTTTTTGCTTCCTCTTGCAAAACCACACTGCTCGACATTGGG
               ******************           *
Clone 9A-3     GGCTTTTTGCTTCCTCTTTAGGGTTAGGGTTAGGGTTAGGGTTA
                    ** *  *     *************************
Tel repeats    TAGGGTTAGGGTTAGGGTTAGGGTTAGGGTTAGGGTTAGGGTTA
```

123 bp deletion, 1 bp homology at addition site

Inversion of chromosome 11

```
pPPT2-tel      AACCACACTGCTCGACTCTGACTCTAGTAGGGATAAGGTTCAGGGTAAT
               *********************              *   *    *    *
Clone 9D-41    AACCACACTGCTCGACTCTGATCTCTTGTTTCCAAGCTTGAGTGTGGCT
                  * *      *    *********************************
Chrom 11       CTGCTCCCAATGCAGGACTGATCTCTTGTTTCCAAGCTTGAGTGTGGCT
```

65 bp inversion, 3 bp homology at fusion site

```
Tel repeats    TTAGGGTTTTAGGGTTAGGGTTAGGGTTAGGGTTAGGGTTAGGG
               *   * *    ***      *   * **********************
Clone 9D-41    TGTTGATCCAGGGGGACTATTCTTGTTTAGGGTTAGGGTTAGGGTTAGG
               *********************************   **
Chrom 11       TGTTGATCCAGGGGGACTATTCTTGTTTAGGGTGCAGGAGGTTCCATAT
```

65 bp inversion, 7 bp homology at telomere addition site

Fig. 2.

DNA sequence analysis of the sites of chromosome healing at the I-*Sce*I-induced DSB in wild type or *Pif1* knockout ES cell lines. The DNA sequences are shown for rare chromosome healing events that did not occur at the site of the I-SceI-induced DSB. Comparisons are shown between the site of chromosome healing in the various Gan^r subclones and the original sequence of the pPPT2-tel plasmid and telomeric repeat sequences (Tel repeats). Homologous nucleotides (*), and mutations or microhomology at the site of telomere addition (bold) are shown. The *Pif1* knockout subclone PIF-9A-3 contained a mixture of two different healing events that occurred near each other following degradation of the DNA at the site of the DSB. The *Pif1* knockout subclone PIF-9D-41 contains an inverted repeat consisting of murine genomic DNA 1275 bp from the plasmid integration site on chromosome 11, which is located between the pPPT2-tel plasmid sequences and the newly added telomere. The size of the deletions or inversion, and the amount of microhomology at the site of telomere addition or fusion is shown for each subclone.

Table 1

Expression of PIF1 in wild type, heterozygous, and homozygous PIF1 knockout ES cell lines

Cell Type	% Exp*
PIF1+/+	
10PWT-3A	0.04
10PWT-7C	0.02
PIF1+/−	
PIF-2A	0.02
PIF-2D	0.03
PIF-3A	0.01
PIF1−/−	
PIF-2H	0.00
PIF-3D	0.00
PIF-9A	0.00
PIF-9D	0.00

*Relative to L19 expression

Table 2

Types of events resulting from DSBs near a telomere in wild type, PIF1 knockout, and NBS1 hypomorphic murine ES cell lines.

Cell type	Clone	Healing[a] (%)	Fusions[b] (%)	Loss[c, d] (%)	Total
WT					
	FA	8 (33)	10 (42)	6 (25)	24
	CP	13 (38)	3** (9)	18 (53)	34
	FB	4 (29)	4 (29)	6 (43)	14
	BA	8 (29)	16 (57)	4 (14)	28
PIF1					
	2H	10 (42)	4* (17)	10 (42)	24
	9A	12 (41)	2* (7)	15 (52)	29
NBS1					
	7C	20 (41)	8 (16)	21 (43)	49
	8H	5 (50)	3 (30)	2 (20)	10

[a] No difference between WT, PIF1, or NBS1 (p=0.3, Fisher's exact test).

[b] WT vs. PIF1 (p=0.003*, α=0.035), WT vs. NBS1 (p=0.07), PIF1 vs. NBS1 (p=0.3).

[c] WT vs. PIF1 (p=0.2), WT vs. NBS1 (p=0.6), PIF1 vs. NBS1 (p=0.4).

[d] No difference within or between groups when loss and fusions combined (p>0.3).

** Fewer fusions than other WT clones (p=0002, α=0.02), no difference to Pif1 (p=1.0).

DNA Repair (Amst). Author manuscript; available in PMC 2012 November 10.

Table 3

Comparison of the location of *de novo* telomere addition at the I-SceI-induced DSB in wild type and PIF knockout ES cell lines.

Healing type	Number of events (%)	
	PIF1+/+	PIF1−/−
Site A	30 (54.5)	26 (47.3)
Site B0	18 (32.7)	17 (30.9)
Site C	2 (3.6)	4 (7.3)
Mutation*	4 (7.3)	5 (9.1)
Deletion	1 (1.8)	3 (5.5)

*Chromosome healing involving alterations in nucleotides at the I-SceI site.